Zika virus NS3 protease and its cellular substrates

Agnieszka Dabrowska[a,b], Aleksandra Milewska[a,b], Joanna Ner-Kluza[c], Piotr Suder[c], Krzysztof Pyrc[a,*]

[a] Virogenetics Laboratory of Virology, Malopolska Centre of Biotechnology, Jagiellonian University, Gronostajowa 7a, 30–387 Krakow, Poland.

[b] Microbiology Department, Faculty of Biochemistry, Biophysics and Biotechnology, Jagiellonian University, Gronostajowa 7, 30-387 Krakow, Poland.

[c] Department of Biochemistry and Neurobiology, Faculty of Materials Science and Ceramics, AGH University of Science and Technology, Mickiewicza 30, 30-059 Krakow, Poland.

[*] Corresponding author

* Correspondence should be addressed to **Krzysztof Pyrc**, Virogenetics Laboratory of Virology, Malopolska Centre of Biotechnology, Jagiellonian University, Gronostajowa 7a, 30-387 Krakow, Poland; Phone number: +48 12 664 61 21; www: http://virogenetics.info, E-mail: k.a.pyrc@uj.edu.pl

ABSTRACT

Zika virus is a flavivirus discovered in 1947, but the association between Zika virus infection and brain disorders was not demonstrated until 2015 in Brazil. Infection mostly poses a threat to women during pregnancy, since it may cause microcephaly and other neurological dysfunctions in the developing fetus. However, infection is also associated with Guillain-Barré syndrome. The nonstructural NS3 protein is essential for virus replication because it helps to remodel the cellular microenvironment. Several reports show that this protease can process cellular substrates and thereby modify cellular pathways that are important for the virus. Herein, we explored some of the targets of NS3, but we could not confirm the biological relevance of its protease activity. Thus, although mass spectrometry is highly sensitive and useful in many instances, being also able to show directions, where cell/virus interaction occurs, we believe that biological validation of the observed results is essential.

INTRODUCTION

Zika virus is a flavivirus discovered in 1947 in primates inhabiting the African Zika forest (1). Although the virus was found to infect humans, for decades it was not considered to be a medical threat due to limited distribution and very mild symptoms associated with infection. However, more than 10 years ago interest in Zika virus began to increase as it became clear that the virus has broadened its geographic distribution, and the first outbreak was reported in the Federated States of Micronesia (2). In 2015, case definition became more precise, and some data suggested that the infection may be more dangerous than previously thought. While the symptoms are relatively mild and include fever, rash, headache, and muscle pain, infection may cause severe sequelae, and it is associated with Guillain-Barré syndrome (3). The infection is most severe in pregnant women, since it interferes with development of the neurological system of the fetus, predominantly resulting in microcephaly. A number of *in vitro* and *in vivo* studies have confirmed these observations (4-10).

Flaviviruses are small, enveloped viruses with positive-strand RNA genome, which is delivered to the target cell as a single-stranded RNA molecule containing a single open reading frame (ORF). This ORF is translated into an immature polyprotein, which is co- and post-translationally cleaved by viral and cellular proteases to yield 10 mature viral proteins; capsid (C), membrane (prM/M), and envelope (E) structural proteins; and seven nonstructural proteins (NS1, NS2A, NS2B, NS3, NS4A, NS4B, and NS5)(11). Cleavage sites processed by the viral serine NS3 protease are located between NS2A/NS2B, NS2B/NS3, NS3/NS4A, and NS4B/NS5. Furin or similar cellular proteases process the prM/M site, while other host cell proteases reportedly cleave C/prM, prM/E, E/NS1, NS1/NS2A, and NS4A/NS4B sites(12). The NS3 protein consists of an N-terminal serine protease domain (~180 amino acids) and a C-terminal region harboring RNA helicase, nucleoside triphosphatase, and 5' RNA triphosphatase activities. The active site of the N-terminal protease contains a His-Asp-Ser

57 catalytic triad. Furthermore, the small nonstructural NS2B protein serves as an NS3 protease
58 cofactor and anchors it to the endoplasmic reticulum (ER) membrane (13-17). The presence or
59 absence of NS2B affects the tertiary structure, activity, and stability of NS3 (18-20).
60 Flaviviral proteases are essential for viral replication, hence they are considered promising
61 targets for antiviral agents. Indeed, the development of HCV NS3/NS4A protease inhibitors
62 proved a breakthrough in hepatitis C therapy, and these drugs received U.S. Food & Drug
63 Administration (FDA) and European Medicines Agency (EMA) approval for use in humans
64 (21-23).
65 Interestingly, flaviviral proteases have also been reported to modify the cellular
66 microenvironment. Cleavage of host proteins may be beneficial for the virus by diminishing
67 the cellular responses, remodeling cellular metabolism, and other mechanisms. Such a strategy
68 is common for viruses, as exemplified by human rhinovirus (HRV) that modulates apoptosis
69 by cleaving receptor-interacting protein kinase-1 (RIPK1) at the noncanonical site, and
70 blocking caspase 8-mediated activation of the pathway (24). Interestingly, the picornaviral
71 protease also processes translation initiation factor eIF4G, part of the cellular translation
72 initiation complex. Targeting of this molecule results in decreased production of cellular
73 proteins but does not affect the production of viral proteins, as picornaviruses use internal
74 ribosome entry sites (IRES) for cap-independent translation. In this way, the viral protease
75 hijacks the cellular protein production machinery (25-27). The NS3/NS4A protease of hepatitis
76 C virus cleaves mitochondrial antiviral signaling protein (MAVS) and TIR domain-containing
77 adapter-inducing interferon-β protein (TRIF) to evade the host cell antiviral response (28-30).
78 Various targets of the Zika virus protease have been identified. FAM134B (family with
79 sequence similarity 134), ATG16L1 (autophagy-related protein 16-1), eIF4G1 (eukaryotic
80 translation initiation factor 4 gamma 1), and Septin-2 are among the most interesting targets.
81 Except for FAM134B, these targets were identified using mass spectrometry methods, which

82 provide unrivalled sensitivity and are capable of cell proteome studies. However, careful
83 analysis of the reported data showed that none of the protein targets are shared between the
84 published studies. Thus, we explored the reported data in detail by employing classical
85 approaches such as western blotting, as well as functional approaches based on the activity of
86 particular pathways. Herein, we present an example of such a study, in which we failed to
87 confirm protease-mediated or virus-related degradation of the eIF4G1 protein. We were also
88 unable to confirm the beneficial effects of decreasing eIF4G1 on viral replication.

MATERIALS AND METHODS

Cell culture

293T cells (ATCC CRL-3216; human embryonic kidney cells), A549 cells (ATCC CCL-185; lung carcinoma cells), Vero cells (ATCC CCL-81; African green monkey kidney cells), and U251 cells (human glioblastoma cell line) were maintained in Dulbecco's modified Eagle's medium (DMEM; Corning, Poland) supplemented with 3% fetal bovine serum (FBS; heat-inactivated; Thermo Scientific, Poland), 100 µg/ml streptomycin, 100 U/ml penicillin (Sigma-Aldrich, Poland), and 5 µg/ml ciprofloxacin. Cells were maintained at 37°C under 5% CO_2.

Virus strains, preparation, and titration

ZIKV H/PF/2013 (acquired from European Virus Archive), ZIKV H/PAN/2016 (BEI resources), ZIKV R116265 Human 2016 Mexico (BEI resources), ZIKV Mosquito Mex 2-81 (BEI resources), ZIKV PRVABC59 (BEI resources), ZIKV MR766 (BEI resources), ZIKV IB H 30656 (BEI resources), ZIKV FLR (BEI resources), ZIKV R103451 Human 2015 Honduras (BEI resources), ZIKV P 6-740 Malaysia 1966 (BEI resources), and ZIKV DAKAR 41524 (BEI resources) strains were employed in this work.

Virus stocks were generated by infection of Vero cells. At 3 days post-infection (p.i.) at 37°C, virus-containing medium was collected and titrated. As a control, mock-infected Vero cells were subjected to the same procedure. Virus and mock aliquots were stored at -80°C. Virus titration was performed on confluent Vero cells in a 96-well plate according to the method described by Reed-Muench(31). Briefly, cells infected with serially diluted virus were incubated at 37°C for 3 days, and the occurrence of a cytopathic effect (CPE) was monitored.

112 **Plasmids**

113 The region encoding the NS2B-NS3^{WT} protein was amplified by PCR using a cDNA
114 template generated from H/FP/2013 Zika virus and appropriate primers (5' ATG CGG TAC
115 CGC CAC CAT GGG CAG CTG GCC CCC TAG CGA A 3'; 5' AGC CGG TAC CCT ATC
116 TTT TCC CAG CGG CAA ACT CC 3'). The resulting product was digested with *Not*I-HF and
117 *Kpn*I-HF (New England Biolabs), gel-purified, and cloned into the pBudCE4.1 vector
118 (pBudCE4.1_NS3^{WT}). The plasmid encoding the inactive NS2B-NS3^{S135A} protease
119 (pBudCE4.1-NS3^{S135A}) was obtained using the pBudCE4.1_NS3^{WT} template by employing the
120 QuickChange PCR technique with appropriate primers (5' GGA ACT GCC GGA TCT CCA
121 ATC CTA GAC AAG 3'; 5' AGA TCC GGC AGT TCC TGC TGG GTA ATC CAG 3') to
122 change the serine residue at amino acid (aa) position 135 to alanine. The obtained plasmids
123 were verified by DNA sequencing.

124

125 **Plasmid transfection**

126 293T cells were maintained as described above. Cells were seeded in 6- or 24-wells plates
127 (TPP, Switzerland) and cultured for 24 h. When 60% confluency was reached, cells were
128 transfected using polyethyleneimine (PEI; Sigma-Aldrich, Poland). For transfection in 6-wells
129 plates, 4 µg plasmid DNA was mixed with 250 µl Opti-MEM medium (Thermo Scientific) and
130 4 µg PEI. For transfection in 24-well plates, 1 µg/well plasmid DNA was mixed with 100 µl
131 Opti-MEM medium with 1 µg PEI. After a 30 min incubation at room temperature, the mixture
132 was added dropwise onto cells. Four hours later, the supernatant was discarded, fresh medium
133 was added, and cells were further incubated at 37°C.

134 A549 cells were maintained as described above. Cells were seeded in 6-wells plates and
135 cultured for 24 h. When 80% confluency was reached, cells were transfected with
136 Lipofectamine 2000 (Thermo Scientific) according to the manufacturer's protocol. Briefly,

2.5 µg plasmid DNA was mixed with 300 µl Opti-MEM medium with 5 µl Lipofectamine 2000. After a 5 min incubation at room temperature, the mixture was added dropwise onto cells. Four hours later, the supernatant was discarded, fresh medium was added, and cells were further incubated at 37°C.

For expression of active and inactive virus protease, pBudCE4.1-NS3^{WT} or pBudCE4.1-NS3^{S135A} plasmids were employed, respectively. For eIF4G1 overexpression, cells were transfected with pcDNA3 HA eIF4GI plasmid or control green fluorescent protein (GFP)-expressing plasmid (pMAX-GFP plasmid, Lonza). pcDNA3 HA eIF4GI (1–1599) was a gift from Nahum Sonenberg (Addgene plasmid #45640; http://n2t.net/addgene:45640; RRID Addgene_45640). The efficiency of expression was verified by western blotting.

siRNA transfection

For small interfering RNA (siRNA) transfection, A549 cells were maintained as described above. Cells were seeded in 24-wells plates, and siRNA was transfected once the confluency reached 80% using RNAiMAX Lipofectamine (Thermo Scientific), according to the manufacturer's protocol. Next, 5 pmol eIF4G1 siRNA (Sigma-Aldrich; Cat. No EHU066831) or control scrambled RNA (Santa-Cruz Biotechnology; Cat. No sc-44237) was mixed in 125 µl Opti-MEM medium containing 3.5 µl transfection reagent. After a 5 min incubation at room temperature, the mixture was added to cells dropwise. The efficiency of eIF4G1 silencing was verified at 24–72 h post-transfection using western blotting.

Virus infection

293T cells, A549 cells, and U251 cells were seeded in 6-wells plates and cultured at 37°C. When 90–100% confluency was reached, cells were inoculated with ZIKV at 2000 $TCID_{50}$/ml for 293T cells or 400 $TCID_{50}$/ml for U251 and A549 cells. Mock cultures were inoculated with

an identical volume of mock samples. All cultures were incubated for 2 h at 37°C under 5% CO_2 in DMEM medium supplemented with 2% FBS, 100 µg/ml streptomycin, and 100 IU/ml penicillin. After incubation, cells were washed twice with phosphate-buffered saline (PBS) and incubated as described above. At 3 days p.i., culture supernatants were collected, viral RNA was isolated, and the yield was quantified by reverse transcription quantitative PCR (RT-qPCR). Also, cells were collected for western blotting analysis.

SUnSET-puromycin assay

A549 and U251 cells were maintained as described above. Cells were seeded in 12-well plates and cultured for 48 h. When 80% confluency was reached, cells were inoculated with the Mexico ZIKV strain at 400 $TCID_{50}$/ml (or an identical volume of the mock culture). Alternatively, 10 µg/ml or 5 µg/ml of the translation inhibitor cycloheximide (CHX; stock solution 100 mg/ml; Sigma-Aldrich) was added to A549 cells and U251 cells, respectively, or 10 µM eIF4G1 inhibitor (4EGI-1; stock solution 10 mM; Biotechne)(32) was added. At 48 h p.i., cells were washed twice with PBS and incubated in unsupplemented DMEM for 2 h at 37°C. The supernatant was discarded, fresh DMEM medium supplemented with 3% FBS, and 1 µM puromycin (stock solution; Merck) was added, and cells were further incubated for 30 min at 37°C. Subsequently, cells were collected for western blotting analysis.

SDS-PAGE and western blotting

Cells grown in 6-well, 12-well, or 24-well plates were lysed for 30 min on ice in 200 µl, 100 µl, or 50 µl RIPA buffer (50 mM TRIS, 150 mM NaCl, 1% Nonidet P-40, 0.5% sodium deoxycholate, 0.1% SDS, pH 7.5), respectively. Subsequently, samples were centrifuged (10 min at 13,000 × g, 4°C), and the pelleted cell debris was discarded. The total protein concentration in each sample supernatant was quantified using the bicinchoninic acid (BCA)

187 method (Pierce BCA Protein Assay Kit; Thermo Scientific) according to the manufacturer's
188 protocol. Supernatants were mixed 5:1 with denaturing buffer (202.5 mM TRIS pH 6.8, 10%
189 SDS, 15% β-mercaptoethanol, 30% glycerol, 0.3% Bromophenol Blue) and boiled at 95°C for
190 5 min.

191 For detection of proteins, lysates were loaded and separated on 12% polyacrylamide gels,
192 and separated by SDS-PAGE over 2 h at 120 V. BlueStar Plus Prestained Protein Markers
193 (NIPPON Genetics, Germany) were used for reference. Subsequently, gels were subjected to
194 wet electrotransfer onto methanol-activated polyvinylidene difluoride (PVDF; GE Healthcare,
195 Poland) membranes in 25 mM TRIS, 192 mM glycine, 20% methanol buffer for 1 h at 100 V.
196 Following transfer, nonspecific binding sites were blocked with 5% skimmed milk (BioShop,
197 Canada) in TRIS-buffered saline (20 mM TRIS, 0.5 M NaCl, pH 7.5) supplemented with 0.05%
198 Tween 20 (TBS-T) by overnight incubation at 4°C. To detect NS3 protein, membranes were
199 incubated with a rabbit anti-NS3 antibody (1:1000, GeneTex, USA) followed by a secondary
200 goat anti-rabbit antibody (1:20000; Dako, Denmark) conjugated with horseradish peroxidase
201 (HRP). To detect the eIF4G1 protein, membranes were incubated with a rabbit anti-eIF4G1
202 antibody (1:1000; Thermo Scientific) followed by a secondary goat anti-rabbit antibody
203 (1:20000; Dako) conjugated with HRP. For puromycin detection, membranes were incubated
204 with mouse anti-puromycin antibody (1:10000; Merck) followed by a secondary rabbit anti-
205 mouse antibody (1:20000; Dako) conjugated with HRP. To detect GAPDH protein, membranes
206 were incubated with a rabbit anti-GAPDH antibody (1:5000; Cell Signaling) followed by a
207 secondary goat anti-rabbit antibody (1:20000; Dako) conjugated with HRP. All antibodies were
208 diluted in 1.5% skimmed milk in TBS-T. The signal was developed using Immobilon Western
209 Chemiluminescent HRP Substrate (Millipore, Poland) and recorded with a ChemiDoc Imaging
210 System (Bio-Rad, Poland).

211

212 **Isolation of nucleic acid and reverse transcription**

213 Viral RNA was isolated from 100 µl cell culture supernatant using a viral DNA/RNA
214 Isolation Kit (A&A Biotechnology, Poland) according to the manufacturer's protocol. Reverse
215 transcription was carried out using a High Capacity cDNA Reverse Transcription Kit (Thermo
216 Scientific) according to the manufacturer's protocol. cDNA samples were prepared in 10 µl
217 volumes using a High Capacity cDNA Reverse Transcription Kit (Thermo Scientific) according
218 to the manufacturer's instructions. The reaction was carried out for 10 min at 25°C, 120 min at
219 37°C, and 5 min at 85°C.

220

221 **Quantitative PCR (qPCR)**

222 Zika virus RNA yields were assessed using real-time PCR on a 7500 Fast Real-Time PCR
223 instrument (Thermo Scientific, Poland). ZIKV cDNA was amplified in a reaction mixture
224 containing 1× TaqMan Universal PCR Master Mix (RT-PCR mix; A&A) in the presence of
225 FAM/TAMRA (6-carboxyfuorescein/6-carboxytetramethylrhodamine) probe (5' CGG CAT
226 ACA GCA TCA GGT GCA TAG GAG 3'; 100 nM) and primers (5' TTG GTC ATG ATA
227 CTG CTG ATT GC 3' and 5' CCT TCC ACA AAG TCC CTA TTG C 3'; 450 nM each). The
228 reaction was carried out for 2 min at 50°C and 10 min at 92°C, followed by 40 cycles at 92°C
229 for 15 s and 60°C for 1 min. DNA standards were subjected to qPCR along with the cDNA.
230 Rox was used as a reference dye.

231

232

RESULTS

Expression of Zika virus protease in eukaryotic cells

In this study, we expressed and purified full-length NS2B-NS3 protein without linkers. The NS2B-NS3 protein and its inactive Ser135Ala variant were expressed from pBudCE4.1 plasmids in 293T (left panel) and A549 (right panel) cells. Western blotting with anti-NS3 antibody (full-length recombinant Zika virus NS3 protein was used as a positive control) detected NS2B-NS3^{WT} and NS2B-NS3^{S135A} in cell lysates prepared from cells collected at 48 h post-transfection. The band corresponding to NS3/NS2B was expected to migrate at ~82 kDa, but the active protease should undergo autocatalytic processing to yield the mature ~68 kDa NS3 protein (**Fig. 1A**). Processing should also result in the generation of the smaller 14 kDa NS2B (**Fig. 1B**). All fragments were observed as expected, confirming the activity of the protease, and protein expression was efficient in both cell lines.

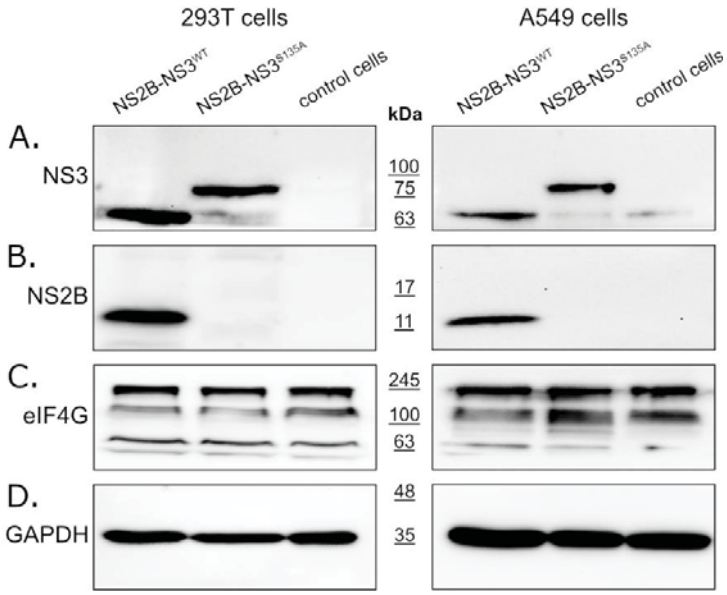

Fig. 1 Expression of active and inactive NS2B-NS3 protease from Zika virus in eukaryotic cells does not affect eIF4G1 protein levels. 293T (left panel) and A549 (right) cells expressing NS2B-NS3^{WT} or NS2B-NS3^{S135A} were assessed alongside control cells. Cells were harvested at 48 h after transfection, lysed, and virus lysates were analyzed by western blotting. Virus infection was confirmed by the presence of NS3 (**A**) and NS2B (**B**) proteins. Anti-eIF4G1 antibody was used to detect and compare changes in eIF4G1 protein abundance in cells expressing active or inactive protease, relative to control cells (**C**). The GAPDH protein was used as a reference to ensure that identical amounts of proteins were present in each sample (**D**).

254

255 **NS3 protease does not affect eIF4G1 levels**

256 To verify whether the ZIKV NS3 protease has any effect on eIF4G1 levels, cells expressing
257 either active or inactive protease were analyzed used western blotting, alongside control cells
258 lacking the protease. The results (**Fig. 1C**) showed that eIF4G1 migrated at ~188 kDa, and
259 isoforms with lower molecular masses were also visible. While we observed high variability in
260 eIF4G1 content depending on the culture time, temperature, and general cell conditions, there
261 were no differences in protein abundance in cells expressing active or inactive protease, or
262 control cells (data not shown), and this was the case for both 293T and A549 cells.

263

264 **Zika virus infection does not result in altered eIF4G1 levels**

265 Since eIF4G1 levels were not affected by the expression of NS3 protease, we assessed
266 whether the eIF4G1 protein is cleaved or degraded during virus infection using ZIKV-infected
267 and mock-infected 293T and A549 cells. First, we confirmed virus replication in cells through
268 NS3 and NS2B protein expression using western blotting **(Fig. 2A, B)**. Levels of the eIF4G1
269 protein were then assessed in virus-infected and mock-inoculated cells, but there were no
270 differences in eIF4G1 protein abundance.

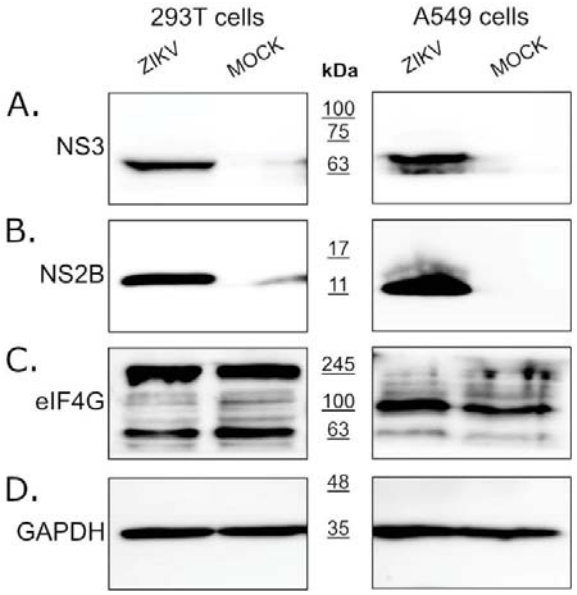

Fig. 2 Expression of the eIF4G1 protein in ZIKV-infected and mock-infected cells. 293T (left panel) and A549 (right panel) cells were infected with ZIKV, or inoculated with mock or virus lysates, and analyzed by western blotting. Virus infection was confirmed by the presence of NS3 (**A**) and NS2B (**B**) proteins. The eIF4G1 protein was detected using anti-eIF4G1 antibody (**C**). The GAPDH protein was used as a reference to ensure that identical amounts of proteins were present in each sample (**D**).

ZIKV does not hamper production of cellular proteins by altering levels of transcription factors

It was suggested that ZIKV NS3 cleaves eIF4G1 to redirect the cellular machinery toward viral protein production, which may be independent of cellular transcription factors(33). To test this hypothesis, the host protein synthesis efficiency was evaluated using surface sensing of translation (SUnSET) assays to measure protein synthesis in cultured cells (34). Puromycin can mimic the aminoacyl end of aminoacyl-tRNAs, and it is partially incorporated in synthesized proteins. The incorporation rate reflects the rate of mRNA translation. Puromycin incorporation was detected by western blotting using anti-puromycin antibodies. Two reference inhibitors were also tested: the protein synthesis inhibitor cycloheximide (CHX) and the eIF4G1-specific inhibitor 4EGI1 **(Fig. 3A)**. In samples treated with either CHX or 4EGI1, the synthesis of proteins was significantly hampered, but protein synthesis in ZIKV-infected cells was not altered. The cytotoxicity of the inhibitors was also evaluated (**Fig. 3B**).

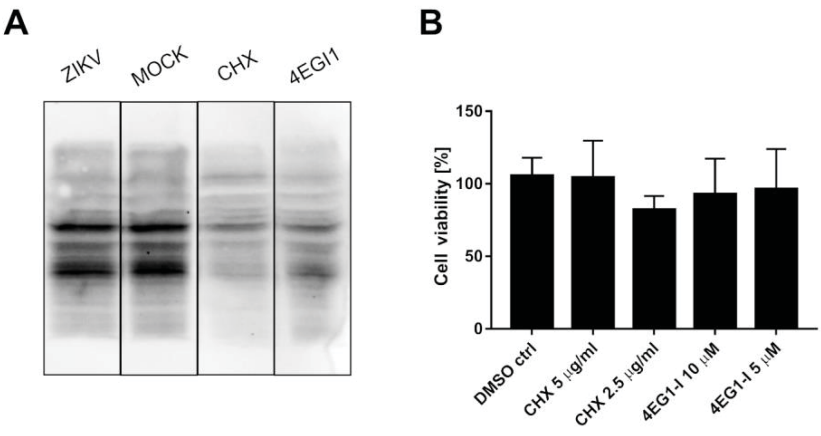

Fig. 3 ZIKV infection does not inhibit the translation of host proteins. SUnSet assays were performed on ZIKV- and mock-infected A549 cells, and cells treated with cycloheximide or 4EGI1 inhibitors. The presence of puromycin protein was detected using anti-puromycin antibody (**A**). Cell viability was evaluated relative to control cells treated with DMSO alone. The assay was performed in triplicate, and average values with standard errors are presented (B).

Overexpression of eIF4G1 does not limit ZIKV replication

To verify whether eIF4G1 expression negatively regulates replication of ZIKV, 293T cells were transfected with a plasmid encoding eIF4G1 (or GFP as a control). Protein levels were verified using western blotting **(Fig. 4A)**, and ZIKV replication was evaluated in non-transfected cells, GFP-expressing cells, and eIF4G-expressing cells. Different strains of Zika virus were used to ensure that any effect is not limited to a single lineage. Cells were infected, and at a single timepoint cell culture supernatants were collected for RNA isolation and subsequent RT-qPCR assessment of the virus yield. Although virus yields varied depending on the virus strain, no inhibition of virus replication was observed for any of the tested strains. These results show that NS3-mediated loss of function of the eIF4G1 protein was not beneficial for virus replication **(Fig. 4B)**.

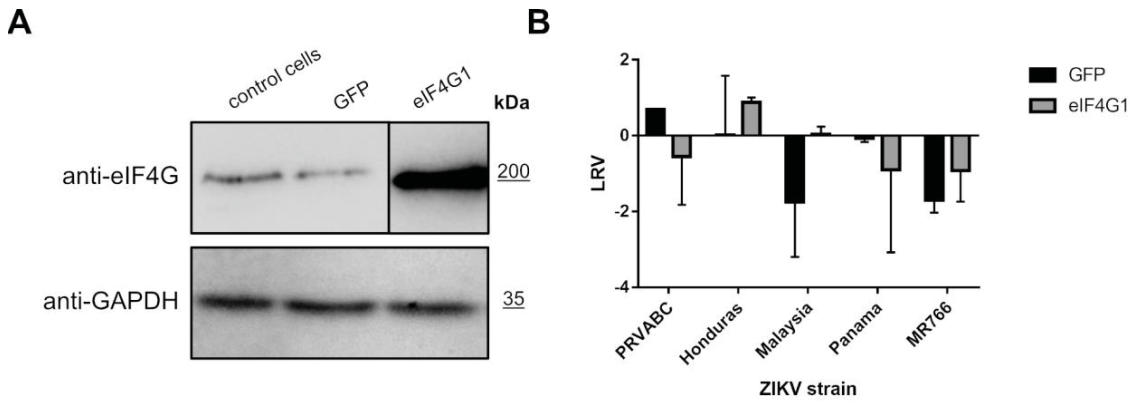

Fig. 4 ZIKV replication in eIF4G1-overexpressing cells. Western blotting analysis (anti-eIF4G1 antibodies) was performed on 293T cells transfected with plasmid encoding eIF4G1 or GFP. The GAPDH protein was used as a reference to ensure that identical amounts of proteins were present in each sample (**A**). ZIKV virus replication in 293T cells transfected with plasmid encoding eIF4G1 or GFP. The virus yield was assessed by RT-qPCR. The y-axis represents the log reduction value (LRV) in virus yield in treated samples, and the x-axis corresponds to different ZIKV strains. The assay was performed in triplicate, and average values with standard errors are presented (**B**).

eIF4G supports replication of ZIKV

To further investigate the role of eIF4G1, we silenced its expression in 293T cells and probed ZIKV replication in these cells. Briefly, cultures were transfected with eIF4G1 siRNA or with scrambled siRNA. Silencing was confirmed by western blotting using antibodies specific to eIF4G1 **(Fig. 5A)**. Cells were infected with ZIKV and incubated for 3 days at 37°C, after which culture supernatants were collected, RNA was isolated and reverse transcribed, and virus replication was evaluated by qPCR. Again, we did not observe an increase in virus production; on the contrary, for some strains, silencing led to inhibition of virus replication relative to control cells or cells transfected with scrambled siRNA **(Fig. 5B)**.

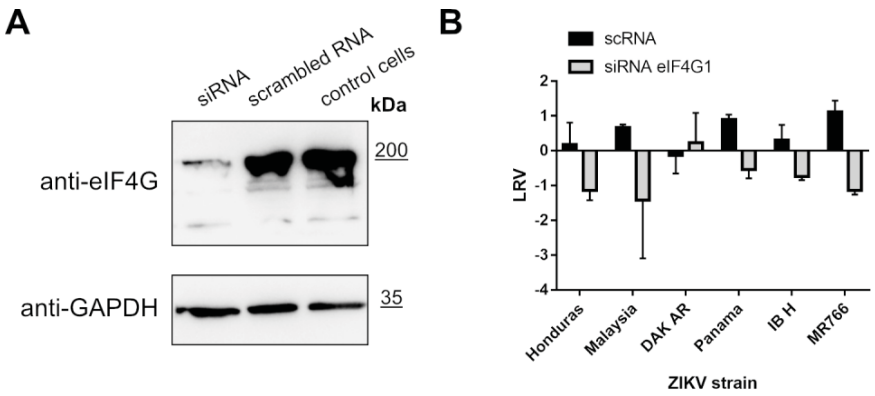

Fig. 5 ZIKV replication in cells lacking eIF4G1. A549 cells were transfected with eIF4G1 siRNA or scrambled siRNA. Non-transfected controls were included. The GAPDH protein was used as a reference to ensure that identical amounts of proteins were present in each sample (**A**). ZIKV virus replication in A549 cells transfected with different siRNAs. The virus yield was assessed by RT-qPCR. The y-axis represents the log reduction value (LRV) in virus yield in treated samples, and the x-axis corresponds to different ZIKV strains. The assay was performed in triplicate, and average values with standard errors are presented (**B**).

Discussion

This study aimed to verify the role of the ZIKV NS3 protein in the remodeling of host cells. NS3 protease is essential for virus replication because it is required for viral protein maturation (35-37). However, viral proteases are generally considered to be highly specific enzymes that co-evolved with the host, and they typically target specific cellular pathways to support viral replication in the host cell, or to block recognition of the virus by the host immune system (38, 39). In the case of ZIKV, some protease targets have been identified, and these are listed in **Table 1**.

345 **Table 1**. Reported NS3 protease targets in the cell.

	PROTEIN	FUNCTION	PROTEASE EXPRESSION	CELLULAR MODEL	IDENTIFICATION	REFERENCES
1	autophagy-related protein 16-1 (ATG16L1)	Autophagy	expression in the prokaryotic system; construct based on 48-100 aa residues of NS2B and 1-178 aa of NS3 (protease domain)	protease substrate verification in the cellular lysate of 293T and A549 cells treated with purified protease;	mass spectrometry; Western blot analysis	(33)
2	eukaryotic translation initiation factor 4 gamma (eIF4G1)	Translation process	expression in prokaryotic system; construct based on 48-100 aa residues of NS2B and 1-178 aa of NS3 (protease domain)	protease substrate verification in cellular lysate of 293T and A549 cells treated with purified protease;	mass spectrometry; Western blot analysis	(33)
3	FAM134B	Reticulofagy	expression in eukaryotic cells; the NS2B-NS3 protein coding region was amplified from cDNA produced from HBMEC infected with ZIKV MR766; cells transfection	HBMEC, U2OS, 293T and HeLa cells	Western blots and the fluorescence microscopy analysis	(40)
4	Septin-2	Cytokinesis	expression in eukaryotic cells, cells transfection, and transduction with lentiviral vectors;	HeLa and 293T cells and human neural progenitor cells	mass spectrometry; Western blots and fluorescence microscopy analysis, pull-down assay	(41)
5	disulfide-isomerase A3 (PDIA3)	ER stress response	Expression in eukaryotic cells, cells transfection; construct based on 48-94 aa residues of NS2B and 1-188 aa of NS3 (protease domain)	293T and A549 cells	mass spectrometry and Western blot analysis	(42)
6	aldolase A (ALDOA)	glycolysis	Expression in eukaryotic cells, cells transfection; construct based on 48-94 aa residues of NS2B and 1-188 aa of NS3 (protease domain)	293T and A549 cells	mass spectrometry and Western blot analysis	(42)
7	Nup98, Nup153 and TPR	Formation of nuclear pore complex	Expression in eukaryotic cells, cells transfection	Huh-7 cells	Western blots and the fluorescence microscopy analysis	(43)

346

347

348 In the present work, we reviewed the published data and verified these potential protease
349 targets experimentally by measuring changes in the levels of potential cellular targets in the
350 presence of active or inactive protease. Since in some cases the localization or specificity of the
351 protease may differ in the absence of other viral proteins, we also measured the levels of
352 potential NS3 targets in ZIKV-infected cells.

353 We employed eIF4G1 as a model protease substrate because we believe that processing of
354 this protein has straightforward consequences for both host cells and virus. The eIF4G protein
355 is involved in the translation process by serving as a eukaryotic translation initiation factor.
356 Together with eIF4A and eIF4E, eIF4G forms the EIF4F multi-subunit protein complex, which
357 recognizes the mRNA cap and facilitates the recruitment of mRNA to the ribosome. eIF4G
358 serves mainly as a linker that forms a scaffold for the complex (44). Interestingly, some viruses
359 are reported to target this protein, and thereby rewire the cellular machinery and switch off
360 cellular protein production. For example, coxsackievirus B3 virus-encoded protease cleaves
361 eIF4G1, but the resulting suppression of cellular translation does not affect viral replication,
362 since picornaviruses utilize the IRES rather than cap-dependent translation initiation (25-27).
363 Consequently, the complete protein production machinery serves viral replication. Similarly,
364 for some flaviviruses, it was postulated that the 5'-untranslated region (5'-UTR) may act as an
365 IRES, and NS3 protease encoded in the flaviviral genome may target cellular translation
366 initiation factors (45).

367 Herein, we first tested whether overexpression of NS2B/NS3 had any effect on levels of
368 the eIF4G1 protein, as reported previously by Hill *et al.* (2018). Notably, the authors of this
369 work performed their analysis using ZIKV protease expressed in a prokaryotic system, which
370 was purified and mixed with cellular lysates from 293T and A549 cells (33). In our current
371 work, we expressed part of the ZIKV genome encompassing the NS2B and NS3 proteins. Our
372 approach allowed us to anchor the NS3 protease in the ER membrane *via* the NS2B cofactor.

Furthermore, using this approach, we were able to monitor whether the protease was active in every experiment because it was autocatalytically (in trans and cis) processing its natural substrate (the NS2B/NS3 junction). The catalytically inactive mutant was used as a negative control. Protein content analysis did not reveal any significant decrease in eIF4G1 protein levels. However, the experimental setup used in the present study may not be entirely appropriate, since it may not accurately recapitulate protease activity and localization during natural viral infection. To ensure that the observed effect was not an artifact, cells were infected with ZIKV, and eIF4G1 levels were measured. Because it remains disputable whether a specific decrease in the level of a particular protein is reflected by changes in signal transduction, we tested the effect of ZIKV infection on the production of cellular proteins using the puromycin assay, with appropriate controls (32)·(46). We did not observe any changes in host gene translation, proving that the effect on eIF4G1 cleavage is not likely to alter the physiology of the cell. However, modulation may occur locally at the replication site, and while it would improve viral replication, the effect on the whole cell may be too subtle to be detected. For this reason, the effect of eIF4G1 on ZIKV replication was tested by gene silencing and gene overexpression experiments, but the role of the eIF4G1 protein in viral replication remained elusive.

As listed in **Table 1**, several proteins have been reported as targets for the ZIKV NS3 protease. Intrigued by the results obtained for the eIF4G1 protein, we explored whether autophagy-related protein 16-1 (ATG16L1), c-Jun amino-terminal kinase-interacting protein 4 (JIP4), mitogen-activated protein kinase kinase kinase 7 (TAK1 or MAP3K7), disulfide-isomerase A3 (PDIA3), heterogeneous nuclear ribonucleoprotein A2/B1 (hnRNP A2/B1), aldolase A (ALDOA) (42), ER-localized reticulophagy receptor FAM134B (40), and septin-2 protein (41) may serve as targets for the NS3 protease. To our surprise, we could not confirm these previous observations, and we considered why this might be the case. First, in these

previous studies, different expression systems and constructs were employed. In some cases, part of the NS2B cofactor was covalently linked to NS3 by a flexible linker. This is relevant, as it has been shown by others that the linker itself may alter the dynamics of the protein and, consequently, the substrate specificity of the protease. Second, the soluble version of the protease is not anchored at the membrane, which may also alter the substrate specificity. Third, the localization of the protease in the ER may limit the number of possible targets, and even proteins that may serve as NS3 substrates in biochemical assays may not be cleaved due to the differential spatial distribution. Finally, although mass spectrometry is sensitive enough to detect even minor changes in protein content, it could in some cases deliver results which are not relevant for the homeostasis of the intracellular environment. Therefore proteome changes detected by MS should be confirmed by other methods, and their biological relevance should be explored, using other approaches.

In conclusion, our study shows that the biological role of the ZIKV NS3 protease may be limited. This may be due to the relatively recent transmission of the virus on a large scale to the human population. It would therefore be interesting to analyze virus evolution in humans in the future, especially changes in the localization and/or substrate specificity of NS3 protease.

Funding

This work was supported by the National Science Centre, Poland, in the form of Grant No. 2016/21/B/NZ6/01307 to K.P and P.S. The funders had no role in study design, data collection and analysis, decision to publish, or preparation of the manuscript.

References

1. Dick, G. W., and Haddow, A. J. (1952) Uganda S virus; a hitherto unrecorded virus isolated from mosquitoes in Uganda. I. Isolation and pathogenicity. *Trans R Soc Trop Med Hyg* 46, 600-618
2. Duffy, M. R., Chen, T. H., Hancock, W. T., Powers, A. M., Kool, J. L., Lanciotti, R. S., Pretrick, M., Marfel, M., Holzbauer, S., Dubray, C., Guillaumot, L., Griggs, A., Bel, M., Lambert, A. J., Laven, J., Kosoy, O., Panella, A., Biggerstaff, B. J., Fischer, M., and Hayes, E. B. (2009) Zika virus outbreak on Yap Island, Federated States of Micronesia. *N Engl J Med* 360, 2536-2543
3. Musso, D., Ko, A. I., and Baud, D. (2019) Zika Virus Infection - After the Pandemic. *N Engl J Med* 381, 1444-1457
4. Campos, G. S., Bandeira, A. C., and Sardi, S. I. (2015) Zika Virus Outbreak, Bahia, Brazil. *Emerg Infect Dis* 21, 1885-1886
5. Uncini, A., Shahrizaila, N., and Kuwabara, S. (2017) Zika virus infection and Guillain-Barré syndrome: a review focused on clinical and electrophysiological subtypes. *J Neurol Neurosurg Psychiatry* 88, 266-271
6. Barbi, L., Coelho, A. V. C., Alencar, L. C. A., and Crovella, S. (2018) Prevalence of Guillain-Barré syndrome among Zika virus infected cases: a systematic review and meta-analysis. *Braz J Infect Dis* 22, 137-141
7. Nascimento, O. J. M., and da Silva, I. R. F. (2017) Guillain-Barré syndrome and Zika virus outbreaks. *Curr Opin Neurol* 30, 500-507
8. Vissoci, J. R. N., Rocha, T. A. H., Silva, N. C. D., de Sousa Queiroz, R. C., Thomaz, E. B. A. F., Amaral, P. V. M., Lein, A., Branco, M. D. R. F., Aquino, J., Rodrigues, Z. M. R., da Silva, A. A. M., and Staton, C. (2018) Zika virus infection and microcephaly: Evidence regarding geospatial associations. *PLoS Negl Trop Dis* 12, e0006392
9. Barreto, M. L., Barral-Netto, M., Stabeli, R., Almeida-Filho, N., Vasconcelos, P. F. C., Teixeira, M., Buss, P., and Gadelha, P. E. (2016) Zika virus and microcephaly in Brazil: a scientific agenda. *Lancet* 387, 919-921
10. Mlakar, J., Korva, M., Tul, N., Popović, M., Poljšak-Prijatelj, M., Mraz, J., Kolenc, M., Resman Rus, K., Vesnaver Vipotnik, T., Fabjan Vodušek, V., Vizjak, A., Pižem, J., Petrovec, M., and Avšič Županc, T. (2016) Zika Virus Associated with Microcephaly. *N Engl J Med* 374, 951-958
11. Fields, B. N., Knipe, D. M., and Howley, P. M. (2013) *Fields virology*, 6th Ed., Wolters Kluwer Health/Lippincott Williams & Wilkins, Philadelphia
12. Hoffmann, H. H., Schneider, W. M., Blomen, V. A., Scull, M. A., Hovnanian, A., Brummelkamp, T. R., and Rice, C. M. (2017) Diverse Viruses Require the Calcium Transporter SPCA1 for Maturation and Spread. *Cell Host Microbe* 22, 460-470 e465
13. Bessaud, M., Pastorino, B. A., Peyrefitte, C. N., Rolland, D., Grandadam, M., and Tolou, H. J. (2006) Functional characterization of the NS2B/NS3 protease complex from seven viruses belonging to different groups inside the genus Flavivirus. *Virus Res* 120, 79-90
14. Chambers, T. J., Grakoui, A., and Rice, C. M. (1991) Processing of the yellow fever virus nonstructural polyprotein: a catalytically active NS3 proteinase domain and NS2B are required for cleavages at dibasic sites. *J Virol* 65, 6042-6050
15. Falgout, B., Miller, R. H., and Lai, C. J. (1993) Deletion analysis of dengue virus type 4 nonstructural protein NS2B: identification of a domain required for NS2B-NS3 protease activity. *J Virol* 67, 2034-2042
16. Lescar, J., Luo, D., Xu, T., Sampath, A., Lim, S. P., Canard, B., and Vasudevan, S. G. (2008) Towards the design of antiviral inhibitors against flaviviruses: the case for the multifunctional NS3 protein from Dengue virus as a target. *Antiviral Res* 80, 94-101
17. Leung, D., Schroder, K., White, H., Fang, N. X., Stoermer, M. J., Abbenante, G., Martin, J. L., Young, P. R., and Fairlie, D. P. (2001) Activity of recombinant dengue 2 virus NS3

473 protease in the presence of a truncated NS2B co-factor, small peptide substrates, and inhibitors.
474 *J Biol Chem* 276, 45762-45771
475 18. Aguilera-Pesantes, D., and Méndez, M. A. (2017) Structure and sequence based
476 functional annotation of Zika virus NS2b protein: Computational insights. *Biochem Biophys*
477 *Res Commun* 492, 659-667
478 19. Erbel, P., Schiering, N., D'Arcy, A., Renatus, M., Kroemer, M., Lim, S. P., Yin, Z.,
479 Keller, T. H., Vasudevan, S. G., and Hommel, U. (2006) Structural basis for the activation of
480 flaviviral NS3 proteases from dengue and West Nile virus. *Nat Struct Mol Biol* 13, 372-373
481 20. Xing, H., Xu, S., Jia, F., Yang, Y., Xu, C., Qin, C., and Shi, L. (2020) Zika NS2B is a
482 crucial factor recruiting NS3 to the ER and activating its protease activity. *Virus Res* 275,
483 197793
484 21. Chatel-Chaix, L., Germain, M. A., Götte, M., and Lamarre, D. (2012) Direct-acting and
485 host-targeting HCV inhibitors: current and future directions. *Curr Opin Virol* 2, 588-598
486 22. Chatel-Chaix, L., Baril, M., and Lamarre, D. (2010) Hepatitis C Virus NS3/4A Protease
487 Inhibitors: A Light at the End of the Tunnel. *Viruses* 2, 1752-1765
488 23. McCauley, J. A., and Rudd, M. T. (2016) Hepatitis C virus NS3/4a protease inhibitors.
489 *Curr Opin Pharmacol* 30, 84-92
490 24. Croft, S. N., Walker, E. J., and Ghildyal, R. (2018) Human Rhinovirus 3C protease
491 cleaves RIPK1, concurrent with caspase 8 activation. *Sci Rep* 8, 1569
492 25. Avanzino, B. C., Fuchs, G., and Fraser, C. S. (2017) Cellular cap-binding protein,
493 eIF4E, promotes picornavirus genome restructuring and translation. *Proc Natl Acad Sci U S A*
494 114, 9611-9616
495 26. Chase, A. J., and Semler, B. L. (2012) Viral subversion of host functions for
496 picornavirus translation and RNA replication. *Future Virol* 7, 179-191
497 27. Glaser, W., and Skern, T. (2000) Extremely efficient cleavage of eIF4G by picornaviral
498 proteinases L and 2A in vitro. *FEBS Lett* 480, 151-155
499 28. Li, K., Foy, E., Ferreon, J. C., Nakamura, M., Ferreon, A. C., Ikeda, M., Ray, S. C.,
500 Gale, M., and Lemon, S. M. (2005) Immune evasion by hepatitis C virus NS3/4A protease-
501 mediated cleavage of the Toll-like receptor 3 adaptor protein TRIF. *Proc Natl Acad Sci U S A*
502 102, 2992-2997
503 29. Meylan, E., Curran, J., Hofmann, K., Moradpour, D., Binder, M., Bartenschlager, R.,
504 and Tschopp, J. (2005) Cardif is an adaptor protein in the RIG-I antiviral pathway and is
505 targeted by hepatitis C virus. *Nature* 437, 1167-1172
506 30. Anggakusuma, Brown, R. J. P., Banda, D. H., Todt, D., Vieyres, G., Steinmann, E., and
507 Pietschmann, T. (2016) Hepacivirus NS3/4A Proteases Interfere with MAVS Signaling in both
508 Their Cognate Animal Hosts and Humans: Implications for Zoonotic Transmission. *J Virol* 90,
509 10670-10681
510 31. REED, L. J., and MUENCH, H. (1938) A SIMPLE METHOD OF ESTIMATING
511 FIFTY PER CENT ENDPOINTS12. *American Journal of Epidemiology* 27, 493-497
512 32. Moerke, N. J., Aktas, H., Chen, H., Cantel, S., Reibarkh, M. Y., Fahmy, A., Gross, J.
513 D., Degterev, A., Yuan, J., Chorev, M., Halperin, J. A., and Wagner, G. (2007) Small-molecule
514 inhibition of the interaction between the translation initiation factors eIF4E and eIF4G. *Cell*
515 128, 257-267
516 33. Hill, M. E., Kumar, A., Wells, J. A., Hobman, T. C., Julien, O., and Hardy, J. A. (2018)
517 The Unique Cofactor Region of Zika Virus NS2B-NS3 Protease Facilitates Cleavage of Key
518 Host Proteins. *ACS Chem Biol* 13, 2398-2405
519 34. Schmidt, E. K., Clavarino, G., Ceppi, M., and Pierre, P. (2009) SUnSET, a
520 nonradioactive method to monitor protein synthesis. *Nat Methods* 6, 275-277

35. Falgout, B., Pethel, M., Zhang, Y. M., and Lai, C. J. (1991) Both nonstructural proteins NS2B and NS3 are required for the proteolytic processing of dengue virus nonstructural proteins. *J Virol* 65, 2467-2475
36. Liu, W. J., Sedlak, P. L., Kondratieva, N., and Khromykh, A. A. (2002) Complementation analysis of the flavivirus Kunjin NS3 and NS5 proteins defines the minimal regions essential for formation of a replication complex and shows a requirement of NS3 in cis for virus assembly. *J Virol* 76, 10766-10775
37. Gebhard, L. G., Iglesias, N. G., Byk, L. A., Filomatori, C. V., De Maio, F. A., and Gamarnik, A. V. (2016) A Proline-Rich N-Terminal Region of the Dengue Virus NS3 Is Crucial for Infectious Particle Production. *J Virol* 90, 5451-5461
38. Castelló, A., Franco, D., Moral-López, P., Berlanga, J. J., Alvarez, E., Wimmer, E., and Carrasco, L. (2009) HIV- 1 protease inhibits Cap- and poly(A)-dependent translation upon eIF4GI and PABP cleavage. *PLoS One* 4, e7997
39. Alvarez, E., Menéndez-Arias, L., and Carrasco, L. (2003) The eukaryotic translation initiation factor 4GI is cleaved by different retroviral proteases. *J Virol* 77, 12392-12400
40. Lennemann, N. J., and Coyne, C. B. (2017) Dengue and Zika viruses subvert reticulophagy by NS2B3-mediated cleavage of FAM134B. *Autophagy* 13, 322-332
41. Li, H., Saucedo-Cuevas, L., Yuan, L., Ross, D., Johansen, A., Sands, D., Stanley, V., Guemez-Gamboa, A., Gregor, A., Evans, T., Chen, S., Tan, L., Molina, H., Sheets, N., Shiryaev, S. A., Terskikh, A. V., Gladfelter, A. S., Shresta, S., Xu, Z., and Gleeson, J. G. (2019) Zika Virus Protease Cleavage of Host Protein Septin-2 Mediates Mitotic Defects in Neural Progenitors. *Neuron* 101, 1089-1098.e1084
42. Tangsongcharoen, C., Roytrakul, S., and Smith, D. R. (2019) Analysis of cellular proteome changes in response to ZIKV NS2B-NS3 protease expression. *Biochim Biophys Acta Proteins Proteom* 1867, 89-97
43. De Jesús-González, L. A., Cervantes-Salazar, M., Reyes-Ruiz, J. M., Osuna-Ramos, J. F., Farfán-Morales, C. N., Palacios-Rápalo, S. N., Pérez-Olais, J. H., Cordero-Rivera, C. D., Hurtado-Monzón, A. M., Ruíz-Jiménez, F., Gutiérrez-Escolano, A. L., and Del Ángel, R. M. (2020) The Nuclear Pore Complex: A Target for NS3 Protease of Dengue and Zika Viruses. *Viruses* 12
44. Jackson, R. J., Hellen, C. U., and Pestova, T. V. (2010) The mechanism of eukaryotic translation initiation and principles of its regulation. *Nat Rev Mol Cell Biol* 11, 113-127
45. Song, Y., Mugavero, J., Stauft, C. B., and Wimmer, E. (2019) Dengue and Zika Virus 5' Untranslated Regions Harbor Internal Ribosomal Entry Site Functions. *MBio* 10
46. Schneider-Poetsch, T., Ju, J., Eyler, D. E., Dang, Y., Bhat, S., Merrick, W. C., Green, R., Shen, B., and Liu, J. O. (2010) Inhibition of eukaryotic translation elongation by cycloheximide and lactimidomycin. *Nat Chem Biol* 6, 209-217